Robust design of turbine blades with friction contacts in the presence of multiple response levels

International Journal of Non–Linear Mechanics 164 (2024) 104770

Contents lists available at ScienceDirect

International Journal of Non-Linear Mechanics

journal homepage: www.elsevier.com/locate/nlm

Robust design of turbine blades with friction contacts in the presence of multiple response levels

Gianmarco Zara *, Erhan Ferhatoglu, Teresa Maria Berruti, Stefano Zucca

Politecnico di Torino, Department of Mechanical and Aerospace Engineering, Corso Duca Degli Abruzzi 24, 10129, Turin, Italy

ARTICLE INFO

Keywords:
Non-unique contact forces
Under-platform dampers
Turbine bladed disks
Nonlinear vibration
Uncertainty quantification
Variability range

ABSTRACT

Dry friction damping is a widely used solution to mitigate vibrations of turbine blades. At design stage, the computation of the forced response of assemblies of bodies in contact (whose relative motion could result in dry friction damping) could give non-unique solutions due to the possibility of having different static equilibria. Infinite possible vibratory levels in a range are hence possible. A desirable condition for designers is to deal with systems whose response boundaries are not far from each other, i.e. with a low scatter in the response. For systems with multiple vibration levels, the notion of robustness (a robust system has a small response scatter, and viceversa), is particularly important.

A robust design is hence needed for such assemblies. Once a design parameter is identified, two possible approaches are possible to accomplish this task.

The so-called manual approach explores a certain number of values of the design parameter belonging to a certain interval, and chooses the most robust configuration among those calculated. This computation could result in a huge effort if the number of considered values of the design parameter is high.

To overcome this issue, a second approach is here proposed. It is based on a Nested Optimization Algorithm (NOA), which consists in two levels of optimization in order to directly find the most robust configuration in the considered range for the design parameter.

In this paper, NOA is applied to a particular test case consisting in a lumped-parameter system simulating three blades with two UPDs interposed among them. Such a system provides the necessary coupling between different contact interfaces necessary to obtain multiple response levels. In addition, it is useful to investigate the mutual interaction among different UPDs.

Results of NOA are presented together with the results of the manual approach in order to give a validation of the double optimization. Dependence of the response scatter from the contact states of the interfaces is also investigated.

1. Introduction

Preventing high cycle fatigue failures caused by vibrations [1] represents a priority task in the field of turbomachinery. Since a full detuning of the natural frequencies of the system with respect to the frequency of the excitation is not always possible, several solutions have been developed over the years to mitigate the vibration amplitude of the blades. In the case of turbine components, intentional implementation of dry friction damping has been successfully performed in order to achieve this goal.

Different solutions include the use of Under-Platform Dampers (UPDs) ([2–4]), ring dampers ([5,6]), mid-span dampers ([7,8]) or the use of shrouds ([9,10]) or blade-root contacts ([11]). UPDs, in particular, are secondary structures in a bladed disk which indirectly couple adjacent blades and take advantage of their relative motion in order to dissipate energy by friction.

Modelling the effect of friction damping on the forced response of bladed disks requires nonlinear solvers with embedded contact models, to model the interaction between adjacent bodies. A very simple and widely used contact model is the Coulomb friction one, where only 1D motion between the two bodies in contact is considered [12,13]. More elaborated models, which ensure a more accurate response, take into account 1D motion with varying normal load [9], 2D [14,15] and 3D [16] motions.

* Corresponding author.
E-mail address: gianmarco.zara@polito.it (G. Zara).

https://doi.org/10.1016/j.ijnonlinmec.2024.104770
Received 15 September 2023; Received in revised form 22 April 2024; Accepted 23 May 2024
Available online 24 May 2024

The most popular method to compute the forced response of systems with contact interfaces is the uncoupled approach ([17]), where static and dynamic equilibria of the system are solved separately. According to this approach, a static analysis is first carried on to compute the static equilibrium of the system before applying the dynamic excitation. Static normal loads on joint interfaces are used as inputs for the dynamic part of the vibratory response problem. The uncoupled approach is widely used because the computation usually converges in a reasonable time.

However, a more recent approach, involving the solution of the static and dynamic equations together, the so-called coupled approach, proved to give more accurate results [18,19]. The increased accuracy of the coupled approach comes with a drawback, in terms of convergence, since multiple dynamic equilibria of the system exist when some of the contacts are in full-stick condition. This is in agreement with Yang et al. [20,21], who, more than twenty years ago, highlighted the uncertainty of contact forces in wedge UPDs when one damper side was fully stuck during vibration. This uncertainty led to multiple forced response levels, associated to the same set of input parameters.

Previous studies on this type of uncertainty have been performed within the contact mechanics community by Klarbring [22]. By analyzing a simple frictional rate problem (i.e. contact states changing due to a change of the external loads), he showed that a critical parameter exists, such that the mechanical behavior of the system changes when the critical parameter changes sign. The influence of this parameter demonstrated that the non-uniqueness of the response is influenced by the friction coefficient and the relative stiffness coupling between normal and tangential dofs.

A coupling between normal and tangential dofs, which can lead to non-uniqueness of the response, may arise also by getting bodies of different materials in contact: this is the typical setting investigated in the contact mechanics community [23–26]. This type of coupling may also arise in case of multiple contact surfaces with different orientation.

This uncertainty phenomenon was more recently numerically investigated in Refs. [27,28], confirming the existence of a variability range in the response, associated to the non-uniqueness of the mean (static) component of tangential force in fully stuck contacts, extending the range of applications from wedge UPDs to other friction damping devices ([27]).

Determination of the boundaries of multiple responses is crucial in the design phase of blade arrays with multiple friction contact surfaces, since the blades should be designed with respect to the maximum vibration amplitude obtained at resonance for different levels of excitation.

The systematic computation of dynamic response boundaries, due to non-uniqueness of the mean (static) tangential force in fully stuck contacts, was performed for the first time by two of the authors of this paper (Ferhatoglu and Zucca) in Ref. [29], by means of an optimization algorithm. This algorithm solves a non-linear constrained optimization problem, where the non-linear constraint is given by the equilibrium equations of the system obtained by means of the Harmonic Balance Method [30], where periodical quantities are approximated as a Fourier series ([31]). Optimization is carried on by minimizing or maximizing an objective function ([32]), which permits to choose, among infinite dynamic solutions for the non-linear constraint, the two solutions of interest (maximum and minimum amplitude of the forced response). The advantage of this approach is the possibility to get a systematic and deterministic computation of the response bounds of mechanical systems with friction contacts, even with a large number of contact points. Ferhatoglu and Zucca [29] demonstrated the method on realistic turbine blades with shrouds contacts and blade-disk interfaces. They successfully captured the forced response boundaries on several case studies - characterized by cyclic symmetry - by using two orthogonal 1D contact models with varying normal load.

A system with multiple response levels is not so appreciated by the designer since it is not very predictable, it is not “robust”. With this logic a dynamic design of the system is here defined “robust” when, in case of multiple response, the difference between the maximum and the minimum dynamic response is the smallest possible. A possible way to perform a robust design is to explore the space of the design parameter of interest in a manual way, by computing the response for all the possible values of the parameter, searching for the value that gives the maximum robustness. The main issue is that this manual search could result in a huge computation time. To overcome this issue, a Nested Optimization Algorithm (NOA) is here proposed to automatically search for the design parameter value that better matches the design requirement of robustness. NOA consists in two levels of optimization: 1) the inner optimization computes the boundaries of the considered dynamic system through the same method proposed in Ref. [30], 2) the outer optimization exploits the boundaries obtained by the inner optimization and the chosen design parameter in order to obtain the configuration with the maximum possible robustness.

The NOA is here tested on a test case with three blades and two interposed UPDs. This system is particularly interesting and meaningful for the presence of different inclined contact surfaces that give the coupling necessary to have multiple response levels with possible mutual effects between dampers. To the best of the authors’ knowledge, the possible interaction between different UPDs has never been investigated in the existing literature.

Once the design parameters for the UPDs were defined, the robustness of the test case is computed by exploring first manually the design space and then by finding directly the optimal solution by NOA.

The paper is organized as follows. In Section 2 the background of the computation of response boundaries for systems with multiple vibratory levels is recapped since it is a relatively new approach in the literature. In Section 3, the general NOA methodology applicable to systems with friction contact interfaces is presented. In Section 4 NOA is applied to a test case and the result of the manual search of the most robust solution, together with the NOA predictions, is presented by putting in evidence how the existence of multiple response levels is correlated to the contact state in the interfaces.

2. Background

In this section, the original optimization algorithm developed in Ref. [29] is described for two reasons.

- The systematic computation of the variability range of the response of mechanical systems with friction contacts, is a relatively new approach in literature and it is worth to describe it in detail.
- It represents the starting point of the Nested Optimization Algorithm developed to support the robust design of mechanical systems with friction contacts.

2.1. Governing equations

The time-domain equilibrium equations of a mechanical system with contact interfaces can be written as

$$\boldsymbol{M}\,\ddot{\boldsymbol{q}}(t)+\boldsymbol{C}\,\dot{\boldsymbol{q}}(t)+\boldsymbol{K}\,\boldsymbol{q}(t)+\boldsymbol{F}_C(\boldsymbol{q},\dot{\boldsymbol{q}},t)=\boldsymbol{F}_{exc}(t) \tag{1}$$

where t is time, $\boldsymbol{M}$, $\boldsymbol{C}$ and $\boldsymbol{K}$ represent the linear system mass, damping and stiffness matrices respectively. $\boldsymbol{q}(t)$ is the vector of generalized coordinates. $\boldsymbol{F}_C(\boldsymbol{q},\dot{\boldsymbol{q}},t)$ and $\boldsymbol{F}_{exc}(t)$ are the vectors of non-linear contact forces due to the contacts and the external excitation. In case of an assembly made of multiple bodies, the $\boldsymbol{M}$, $\boldsymbol{C}$ and $\boldsymbol{K}$ matrices are block-diagonal, with each block corresponding to one body, while $\boldsymbol{q}$ and $\boldsymbol{F}$ vectors contain degrees of freedom (dofs) and forces of the entire assembly. Using the Harmonic Balance Method (HBM), it is possible to switch to frequency domain

$$\left(-(h\omega)^2\boldsymbol{M}+ih\omega\boldsymbol{C}+\boldsymbol{K}\right)\widehat{\boldsymbol{q}}^h+\widehat{\boldsymbol{F}}_C^h-\widehat{\boldsymbol{F}}_{exc}^h=0\quad h=(0,\ldots,N_h) \tag{2}$$

where $\widehat{\boldsymbol{q}}^h$, $\widehat{\boldsymbol{F}}_C^h$, $\widehat{\boldsymbol{F}}_{exc}^h$ are the Fourier coefficients of the response, contact and external forces respectively. Equilibrium equations are coupled by means of the contact forces $\widehat{\boldsymbol{F}}_C^h = \widehat{\boldsymbol{F}}_C^h(\widehat{\boldsymbol{q}}^0, \ldots, \widehat{\boldsymbol{q}}^{N_h})$. In order to compute the Fourier coefficients of contact forces $\widehat{\boldsymbol{F}}_C^h$ in Eq. (2), a contact model is necessary. In this paper the 1D contact model with varying normal load, depicted in Fig. 1 is used.

According to the proposed model, the contact force is divided in a tangential component $T(t)$ and a normal component $N(t)$ with respect to the contact surface. The model includes a Coulomb slider in tangential direction and two linear springs in both normal and tangential direction (which stiffnesses are k_n and k_t, respectively). The variable $w(t)$ describes the slider position and together with the normal $v(t)$ and tangential $u(t)$ displacement, determines the entity of normal and tangential force for every time instant.

$$N(t) = \max(k_n v(t), 0)\ T(t) = \begin{cases} k_t[u(t) - w(t)] & \textit{stick state} \\ \mu N(t) sign(\dot{w}(t)) & \textit{slip state} \\ 0 & \textit{lift} - \textit{off state} \end{cases} \tag{3}$$

Computation of the tangential force $T(t)$ is not possible in a direct way, since the slider position $w(t)$ is not known in advance. Hence, computing tangential force is performed by a predictor-corrector algorithm, whose steps are detailed in Ref. [10].

The solution of the nonlinear balance equations (Eq. 2) is here performed with the iterative Newton-Raphson method. At each iteration, a vector $\widehat{\boldsymbol{q}}^h (h = 0, \ldots, N_h)$ of unknowns is provided and Fourier coefficients of relative displacements are computed. Then, at each contact the Alternating Frequency/Time (AFT) method ([33]) is used (Fig. 2). In detail, time domain relative displacements u(t) and v(t) are computed by means of Inverse Fast Fourier Transform (IFFT), periodic contact forces T(t) and N(t) are computed by means of the contact model and finally Fourier coefficients of contact forces are computed through a Fast Fourier Transform (FFT). Eventually, the vector $\widehat{\boldsymbol{F}}_C^h$ is assembled and used in Eq. (2).

Within the AFT scheme, the calculation of the periodic contact forces in time domain by means of Eq. (3), requires that the initial value of the tangential contact force $T(0)$ is guessed by the user. In the present work the following expression is used:

$$T(0) = \alpha \mu N(0) \tag{4}$$

where the value $T(0)$ is defined as proportional to the Coulomb limit $\mu N(0)$, where the coefficient $\alpha \subset [-1, 1]$ simulates possible different initial conditions.

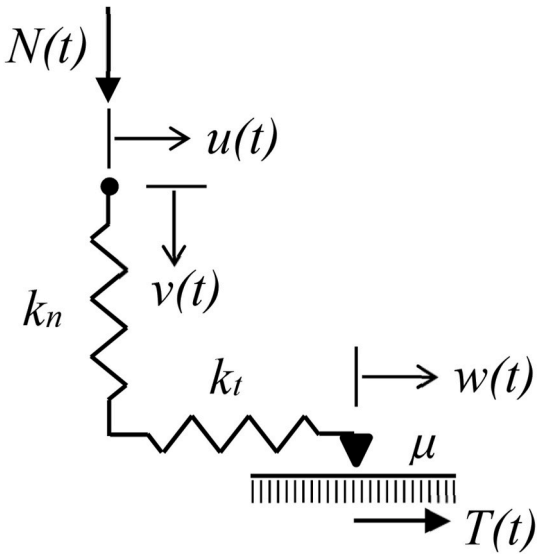

Fig. 1. 1D contact model with varying normal load.

2.2. Non-unique contact forces and multiple responses

When the contact model is used, within the Newton-Raphson iterative solution process, to compute the periodic contact forces $T(t)$ and $N(t)$, one of the possible contact configurations is the so-called full-stick state, characterized by a perfectly elastic behavior of the contact both in tangential and normal direction.

In the full-stick state, the periodic tangential force $T(t)$ is bounded by the upper and lower Coulomb limits and, as shown in Fig. 3, for a given contact kinematics, multiple T(t) curves, characterized by different mean values, can respect the Coulomb inequalities $-\mu N(t) \le T(t) \le \mu N(t)$. The maximum (T^0_{max}) and the minimum (T^0_{min}) admissible mean values correspond to the tangent curves, at given time t, to the upper Coulomb limit curve and to the lower Coulomb limit respectively. All the possible T(t) curves are admissible and each of them is characterized by a specific value of the α coefficient, that determines the corresponding initial condition (Eq. (4)).

In detail, within the AFT process described in Section 2.1, for a given set of periodic relative displacements $u(t)$ and $v(t)$, that result in a full-stick state of the contact, it is possible to obtain any of the admissible $T(t)$ curves, by selecting different initial conditions $T(0)$. Each initial condition corresponds to a value of the α coefficient, defined in Eq. (4).

A clear example of the effect of different values of the α coefficient is provided in Fig. 4, where the four plots correspond to four possible periodic contact forces due to the same periodic relative displacements $u(t)$ and $v(t)$. In all the four cases, the AFT process is performed over two periods, in order to reach a periodic solution (full lines) also when the initial condition does not belong to the periodic curve.

In case (a), the value of the α coefficient $(\alpha_1 = 0.3143)$ allows to obtain the maximum periodic tangential force $T_{max}(t)$ associated to the maximum T^0 value (T^0_{max} in Fig. 3). Since the initial condition already belongs to the final periodic curve, the periodic solution with the AFT process is already obtained during the first period.

In case (b), the value of the α coefficient is larger $(\alpha_2 = 0.75)$ than in the previous case and, after a partial saturation of the tangential force during the first period $(T(t) = \mu N(t))$, the steady-state periodic force $T(t)$, established during the second period, is equal to case (a), showing that the $T_{max}(t)$ curve will be obtained with any $\alpha \in [\alpha_1, 1]$.

Finally, in case (c), a value of $\alpha_3 = 0$, allows obtaining a periodic tangential force $T(t)$ different from those computed in the previous two cases and characterized by a lower value of the average tangential force T^0.

In analogy with case (a), there is a negative value of $\alpha = \alpha_4 < \alpha_3$, that implies negative saturation of the tangential force during the first period $(T(t) = -\mu N(t))$, so that the $T_{min}(t)$ curve will be obtained with any $\alpha \in [-1, \alpha_4]$. Such a situation is represented by case (d), where α_4 is equal to -0.8377.

The existence, in stick condition, of possible different average values of the tangential force suggests that, in a more complex system with multiple contacts, there might be different static equilibria of the system, which are all admissible.

Systems with multiple contacts can be classified as.

a) Systems with no full stick contacts
b) Systems with at least one full stick contact

In type a) systems, every contact has a well-defined hysteresis cycle, this leads to a unique static and dynamic balance conditions.

Systems with at least one full stick contacts are furtherly classified in.

b1) Systems with all full stick contacts

$$\widehat{\boldsymbol{q}}^h \longrightarrow \hat{u}^h, \hat{v}^h \xrightarrow{\text{IFFT}} u(t), v(t) \xrightarrow[\text{Model}]{\text{Contact}} T(t), N(t) \xrightarrow{\text{FFT}} \hat{T}^h, \hat{N}^h \longrightarrow \widehat{\boldsymbol{F}}_c^h$$

Fig. 2. Alternating frequency/time approach.

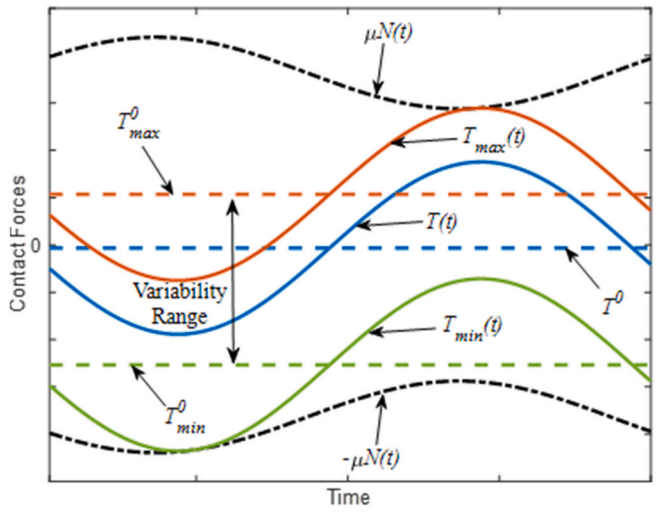

Fig. 3. Time histories of contact forces for a full stick cycle.

b2) Systems with at least a contact that alternates stick-slip or stick-slip-separation

Type b1) systems are structures where infinite static equilibria are possible, but the dynamic response is unique.

Type b2) systems are the key focus of the paper. Multiple mean values of the static tangential contact force for stick contacts implies different static equilibrium of the assembly.

If the static equilibrium of the assembly is not unique, even the static normal force on contacts alternating stick and slip (and separation) can assume multiple values. For stick/slip contacts, the hysteresis cycle and hence the energy dissipated depends on the static normal load. Different levels of energy dissipated by the system, result in multiple vibratory levels.

By following the procedure described in Section 2.1, response computation of a generic structure with N_{cont} contact interfaces needs an array of coefficients as input.

$$\boldsymbol{\alpha} = [\alpha_1, \ldots, \alpha_{N_{cont}}] \tag{5}$$

These coefficients are additional inputs of the system, since their value can affect the system response. Specifically, response of type a) systems is not affected by the values of $\boldsymbol{\alpha}$. In type b1) structures, each static configuration is described by a specific vector $\boldsymbol{\alpha}$, even if a unique dynamic solution exists. On the contrary, in case of type b2) structures, multiple $\boldsymbol{\alpha}$ vectors, imply multiple static and dynamic equilibria.

2.3. Response boundaries and optimization algorithm

In Section 2.2 it was established that, under specific hybrid conditions (some contacts are in full-stick, while other contacts alternate stick-slip) multiple dynamic equilibrium conditions exist. From the engineering point of view, the most relevant configurations among the admissible ones are those leading to the maximum and the minimum response on the system (i.e. the response boundaries).

Ferhatoglu and Zucca [29] developed an optimization algorithm, which found the response boundaries of the system, by maximizing or minimizing the loss factor of the system. The algorithm is briefly described below, since it is used also for the analyses performed in Section 3.

In general, in case of periodic vibration of systems with friction contacts, the loss factor ([34]) is defined as follows

$$\eta = \frac{\Delta W_{diss}}{2\pi U_{pot}} \tag{6}$$

ΔW_{diss} is composed by a linear term ΔW_{visc} (which represents the energy dissipated by viscous damping) and a term due to contact ΔW_{fric} (energy loss due to the contact).

$$\Delta W_{diss} = \Delta W_{visc} + \Delta W_{fric} \propto (h\omega)\widehat{\boldsymbol{q}}^H \boldsymbol{C}\, \widehat{\boldsymbol{q}} + \omega\, \Im\left(\widehat{\boldsymbol{q}}^H\, \widehat{\boldsymbol{F}}_C\right) \tag{7}$$

U_{pot} is the potential energy of the system, that is the sum of the potential energy of the linear system and the potential energy of the contacts

$$U_{pot} = U_{lin} + U_{cont} \propto \widehat{\boldsymbol{q}}^H \boldsymbol{K}\, \widehat{\boldsymbol{q}} + \Re\left(\widehat{\boldsymbol{q}}^H\, \widehat{\boldsymbol{F}}_C\right) \tag{8}$$

As in Ref. [29], maximum and minimum response of a vibrating structure can be systematically computed, by respectively minimizing or maximizing the loss factor. In this way, two different non-linear constrained optimization problems are defined in Table 1.

Where $\boldsymbol{R}$ is the residual of the equilibrium equations

$$\boldsymbol{R} = \left(-(h\omega)^2 \boldsymbol{M} + ih\omega \boldsymbol{C} + \boldsymbol{K} \right) \widehat{\boldsymbol{q}}^h + \widehat{\boldsymbol{F}}_C^h - \widehat{\boldsymbol{F}}_{exc}^h \quad (h = 0, 1, \ldots, H) \tag{9}$$

Both problems in Table 1 correspond to the solution of an extended version of the canonical dynamic system whose unknowns are only the generalized coordinates. In this case the additional unknowns are the previously described α coefficients (Eq. (5)). The solution of the two problems described in Table 1 is performed by the standard Matlab function *fmincon for optimization problems*; in particular the maximum response was obtained by minimizing η and the minimum response by minimizing $-\eta$.

In the present work the response of the system is computed by considering only the 0-th and the 1-st harmonics, although, in the case where higher harmonics are not negligible - e.g. systems where separation occurs - the procedure could be extended to a higher harmonic number.

If a system has not multiple solution (system named a) and b1) in the previous section), the two optimization problems of Table 1 solved with *fmincon* give the same solution.

3. Robust design methodology

The methodology described below exploits and expands the algorithm presented in the previous section for a "robust" design of systems with friction contacts. In this frame, a design can be considered “robust” when, in case of multiple response, the difference between the maximum and minimum response is the smallest possible. The proposed methodology consists in defining the quantity "robustness" and searching the value of design parameters that maximize the robustness in an optimized way by avoiding repeated computations as the design parameters change.

3.1. Robustness definition

A mechanical system with friction contacts, whose nonlinear response is characterized by multiple response levels, is considered. If the optimization algorithm described in Section 2 is used to compute the system response, a plot similar to Fig. 5 is obtained, where the maximum and the minimum responses of the system are shown.

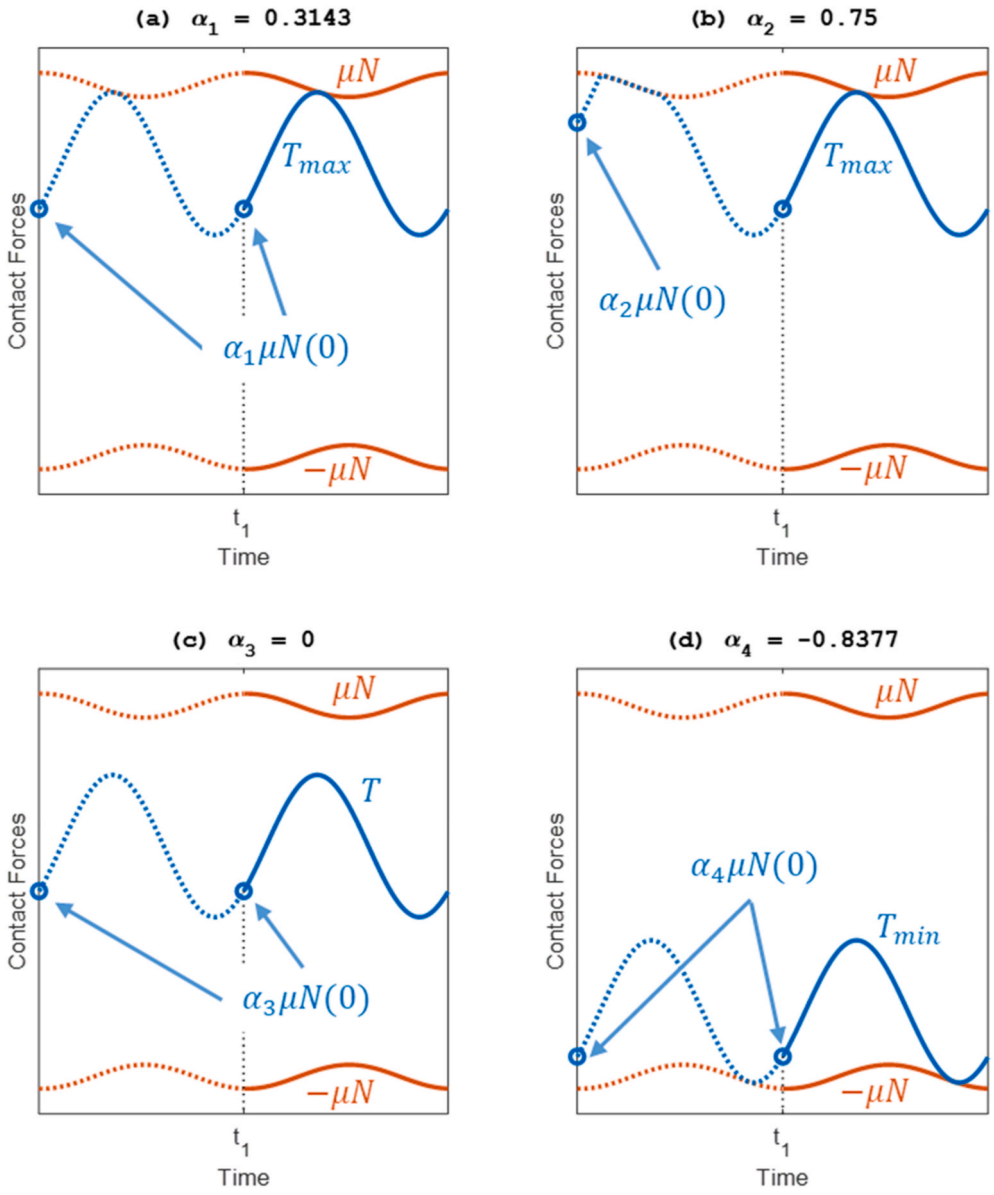

Fig. 4. Contact Forces Time Histories for a full-stick contact (a) $\alpha_1 = 0.3143$, (b) $\alpha_2 = 0.75$, (c) $\alpha_3 = 0$, (d) $\alpha_4 = -0.8377$.

Table 1
Non-linear constrained optimization problems.

Minimum Response	
Maximize	η
With respect to	$[\hat{\boldsymbol{q}}, \boldsymbol{\alpha}]$
Subject to	$\boldsymbol{R} = 0$
Maximum Response	
Minimize	η
With respect to	$[\hat{\boldsymbol{q}}, \boldsymbol{\alpha}]$
Subject to	$\boldsymbol{R} = 0$

The response scatter δ (Fig. 5) between the response bounds at the resonance frequency represents a metric of the uncertainty of the nonlinear forced response. As a consequence, in this paper robustness is defined as

$$R = 1 - \frac{\delta}{y_{max}} \tag{10}$$

As a result, $R = 0$ when the scatter is maximum ($\delta = y_{max}$), and $R = 1$ when the response is unique ($\delta = 0$).

Obtaining a robust system (large value of R) is a desirable condition, since it implies a small response scatter δ corresponding to a more predictable system.

3.2. A nested optimization algorithm for robust design

In general, a design process implies that (at least) one of the parameters of the system is selected as the design parameter p and that the design value, that better matches the design requirements, is searched within a given interval.

The search for the design value can be performed in a manual way, actually exploring the parameters space. If this approach is applied to maximize the robustness of a mechanical system with friction contacts, the optimization process described in Section 2 should be performed at many values of p, within the selected interval. In this way, the response scatter δ and the robustness R could be derived from the maximum and minimum responses computed at each value of p, allowing the designer to eventually select the design value.

To overcome the bottleneck represented by the large amount of

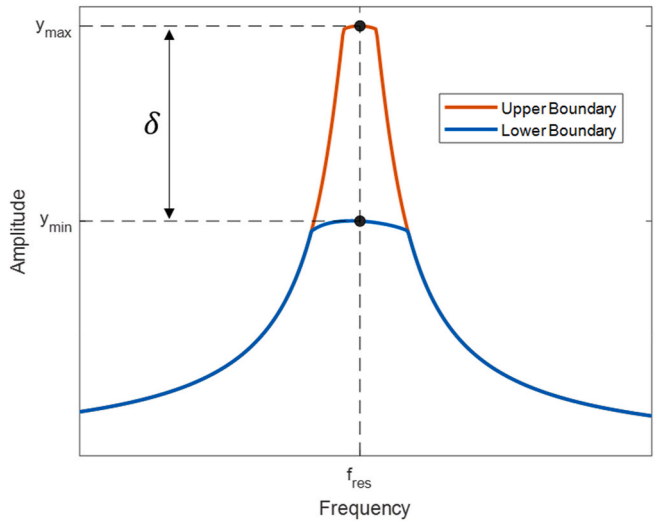

Fig. 5. Typical response scatter of a dynamic system with friction contacts.

calculations and memory that the manual approach implies, a Nested Optimization Algorithm (NOA) is here proposed to automatically search for the design value of p, that matches the design requirements.

The proposed method is a two-level algorithm, depicted in Fig. 6 for the generic design parameter p. It assumes that a reference frequency is selected by the user and that the optimization process is performed at that frequency. Given the nature of the dynamic problems under analysis, a reasonable choice would be a frequency $\omega = \omega_{ref}$ around resonance.

In the NOA, two configurations are defined.

- Configuration #1: maximum response and minimum loss factor (η_1) at $\omega = \omega_{ref}$.
- Configuration #2: minimum response and maximum loss factor (η_2) at $\omega = \omega_{ref}$.

Configuration #1 is characterized by a set of parameters $[\widehat{\boldsymbol{q}}_1, \boldsymbol{\alpha}_1]$, that respect the balance equation of the system $R(\widehat{\boldsymbol{q}}_1, \boldsymbol{\alpha}_1) = 0$. Configuration #2 is characterized by a set of parameters $[\widehat{\boldsymbol{q}}_2, \boldsymbol{\alpha}_2]$, that respect the balance equation of the system $R(\widehat{\boldsymbol{q}}_2, \boldsymbol{\alpha}_2) = 0$.

In the optimization algorithm described in Section 2, the objective function is the loss factor η, therefore, by using the strategy described in Table 1, the minimum (η_1) and maximum (η_2) loss factors can be independently computed for a given value of the design parameter p.

In the proposed NOA, the two above mentioned optimization processes, that search for configurations #1 and #2, are considered as inner optimization problems nested inside an outer optimization procedure, that searches the set of parameters $[\widehat{\boldsymbol{q}}_1, \boldsymbol{\alpha}_1, \widehat{\boldsymbol{q}}_2, \boldsymbol{\alpha}_2, p]$ that minimize the difference $\eta_2 - \eta_1$ and simultaneously respect the balance equations $R(\widehat{\boldsymbol{q}}_1, \boldsymbol{\alpha}_1) = 0$ and $R(\widehat{\boldsymbol{q}}_2, \boldsymbol{\alpha}_2) = 0$.

At the nth iteration the NOA receives as an input a vector of parameters $[\widehat{\boldsymbol{q}}_1, \boldsymbol{\alpha}_1, \widehat{\boldsymbol{q}}_2, \boldsymbol{\alpha}_2, p]_n$ and provides as an output a vector of parameters $[\widehat{\boldsymbol{q}}_1, \boldsymbol{\alpha}_1, \widehat{\boldsymbol{q}}_2, \boldsymbol{\alpha}_2, p]_{n+1}$, that satisfy the inner optimization problems. The optimization loop ends when the minimum value of $(\eta_2 - \eta_1)$ is reached.

4. Numerical test case

The NOA is applied to a test case consisting of 3 blades with 2 interposed UPDs for the following reasons.

- UPDs are common damping devices in turbomachinery blades
- UPDs provide the geometric coupling necessary to have the multiple response levels
- The presence of 2 UPDs in the model allows for investigating their mutual effect on the dynamic response of the system

Both blades and UPDs are modeled as vibrating masses, connected together by springs. The baseline configuration of this system is described in Section 4.1, the design parameters are introduced in Section 4.2 and numerical results are given in Sections 4.3-4.5.

4.1. Baseline system

The model under investigation (Fig. 7) has 10 dofs, since each of the five bodies can move along both x and y axis. The blade masses m are one order of magnitude larger than the damper masses m_D. Each mass m is constrained to the ground with stiffnesses k and viscous dampers c (for simplicity of drawing, viscous dampers are not shown in the picture) in

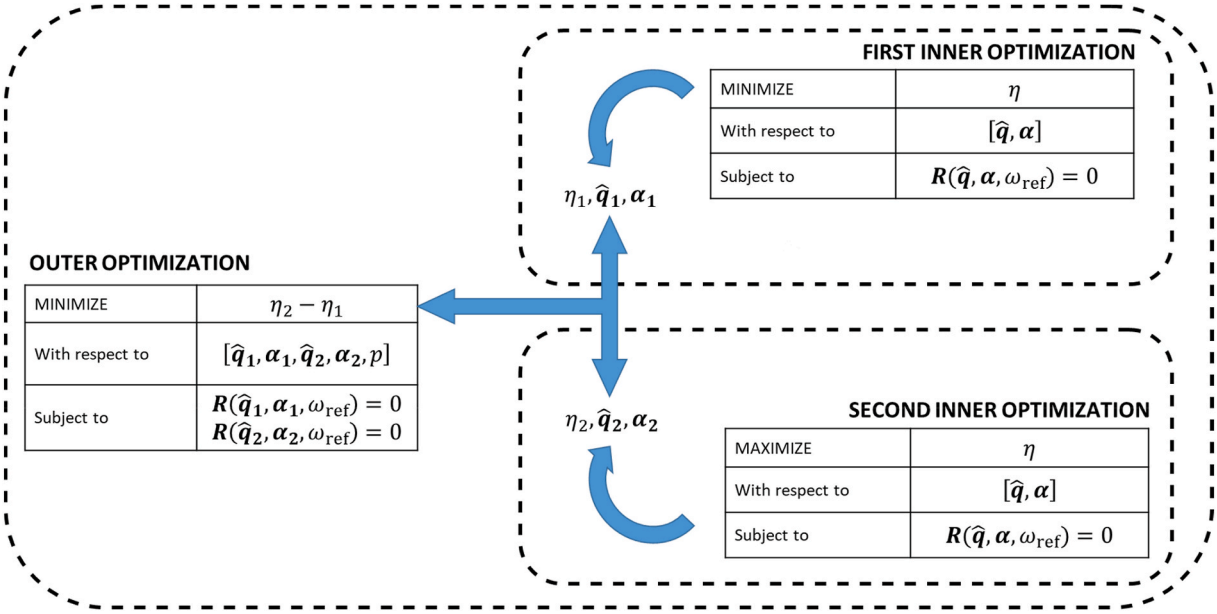

Fig. 6. Definition of the nested optimization algorithm (NOA).

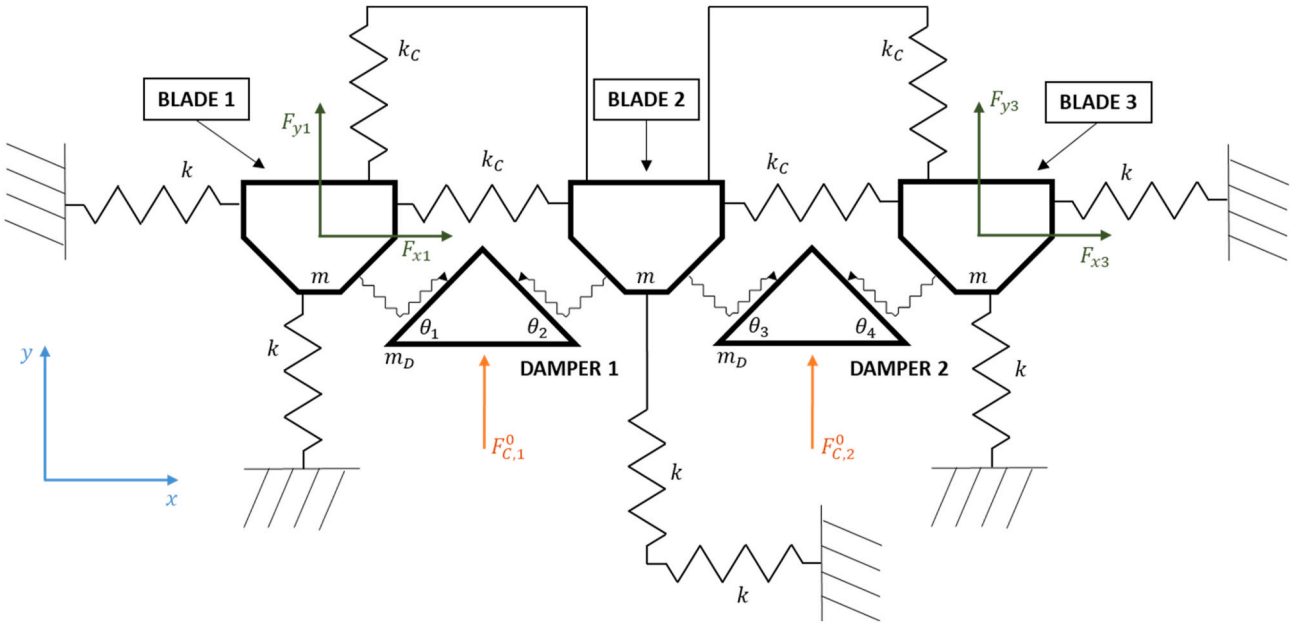

Fig. 7. Case Study lumped parameter System.

order to model the coupling between the blades and the disk. UPDs are wedge dampers, modeled as free rigid bodies; in order to avoid numerical problems, a very low negligible stiffness k_D (not depicted in figure) has been added to constrain the two masses m_D to the ground. Each blade is coupled to the adjacent blades through a stiffness k_C. The vectors of the displacements and the forces are

$$q = \{ x_1 \quad y_1 \quad x_2 \quad y_2 \quad x_3 \quad y_3 \quad x_{D1} \quad y_{D1} \quad x_{D2} \quad y_{D2} \}^T$$

$$F_{exc} = \{ F_{x1} \quad F_{y1} \quad F_{x2} \quad F_{y2} \quad F_{x3} \quad F_{y3} \quad 0 \quad 0 \quad 0 \quad 0 \}^T$$

The values of the lumped parameters are listed in Table 2.

A close-up of the dampers is shown in Fig. 8, where tangential and normal forces are highlighted (left) as well as relative tangential and normal displacements (right) used as inputs of the corresponding contact elements.

The geometry of the UPD is fully defined by the basis angles θ_n. In the baseline configuration all the $\theta_n (n = 1, 2, 3, 4)$ are equal to $\pi/4$ rad. The only external force acting on each damper is a static vertical preload which simulates the centrifugal force, that keeps the damper in contact with the blade platforms during the disk rotation.

The contact parameters of the contact elements, that couple each damper side to the adjacent blade, are: $k_t = 3 \times 10^5\ N/m$, $k_n = 3 \times 10^5\ N/m$, $\mu = 0.5$.

4.1.1. Linear response

Before performing the non-linear analysis, two different linear systems are considered. They represent limit conditions of the contacts, and therefore two limit conditions for the response. The first system is the so-called free system, without the dampers. The second system is the full-stick system, where all the blade-damper contacts are in full-stick condition, due to the presence of linearized contact elements (no slip, no separation) between the blades and the dampers.

Table 2
Lumped parameters values.

Parameter	Value	Parameter	Value
m	$1\ kg$	k	$3 \times 10^5\ Nm^{-1}$
m_D	$1 \times 10^{-1}\ kg$	k_C	$7 \times 10^5\ Nm^{-1}$
c	$20\ Nsm^{-1}$	k_D	$3 \times 10^3\ Nm^{-1}$

The natural frequencies of the free and full-stick system are shown in Table 3. Due to the symmetry of both systems, pairs of identical natural frequencies are found.

Due to the presence of the dampers, the full-stick system is generally stiffer than the free system, resulting in higher values of its natural frequencies. A very slight softening effect due to the mass of the dampers is only observed in the first 2 natural frequencies, corresponding to in-phase vibration of the 3 blades, since no relative displacement occurs between adjacent masses.

As shown in Table 3, the natural frequencies of modes #5 and #6, corresponding to the out-of-phase vibration of blades #1 and #3, are those more affected by the introduction of the damper, making them the suitable target for the nonlinear forced response analysis.

It was then chosen to impose a vector of periodic external forces that highly excite that specific mode shapes, as shown in Table 4.

4.1.2. Non-linear response

The nonlinear forced response of the baseline system is then performed assuming evenly distributed static forces on the dampers ($F^0_{C,1} = F^0_{C,2} = F^0_{C,ref} = 150\ N$).

The maximum and the minimum responses of the system are computed with the optimization algorithm described in Section 2. The vertical displacement y_2 of blade 2 is shown in Fig. 9, together with the free and full-stick response as references.

The nonlinear responses obtained by the analysis confirm that the values of pre-load and harmonic forces selected allow the damper to dissipate energy by friction, thus reducing the maximum vibration amplitude with respect to the full-stick case, without significant changes in the resonance frequency. Moreover, the optimization algorithm found the response bounds (i.e maximum and minimum responses), showing that a scatter δ in the response exists, making this test case suitable for a robust design analysis.

In Fig. 10, the time histories of the contact forces are shown for both minimum and maximum response at a frequency near the full-stick resonance (267 Hz).

In both cases, each damper has one interface in full-stick and the other alternating stick and slip. In particular inner contacts (2 and 3) are in full-stick, while outer contacts (1 and 4) alternate stick-slip. Each damper is a b2)-like structure as defined in Section 2.2, since they both have one full stick side and the other one alternating stick and slip. This

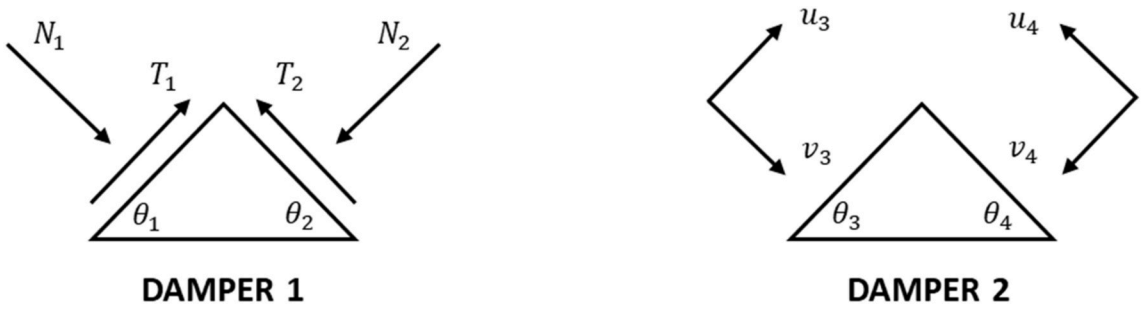

Fig. 8. View of the damper 1 with contact forces and the damper 2 with local relative displacements.

Table 3
Free and Full stick systems – Natural Frequencies.

Mode #	Natural frequencies [Hz]		Mode shape
	Free	Full stick	
1	87.17	84.58	System mode
2	87.17	84.58	System mode
3	159.15	168.19	System mode
4	159.15	168.19	System mode
5	246.56	266.89	System mode
6	246.56	266.89	System mode
7		396.71	Damper mode
8		396.71	Damper mode
9		406.88	Damper mode
10		406.88	Damper mode

Table 4
Excitation forces for forced response analysis.

Parameter	Value	Parameter	Value
$F_{x,1}$	$5\cos(\omega t)$ N	$F_{y,1}$	$20\cos(\omega t)$ N
$F_{x,2}$	0	$F_{y,2}$	0
$F_{x,3}$	$-5\cos(\omega t)$ N	$F_{y,3}$	$20\cos(\omega t)$ N

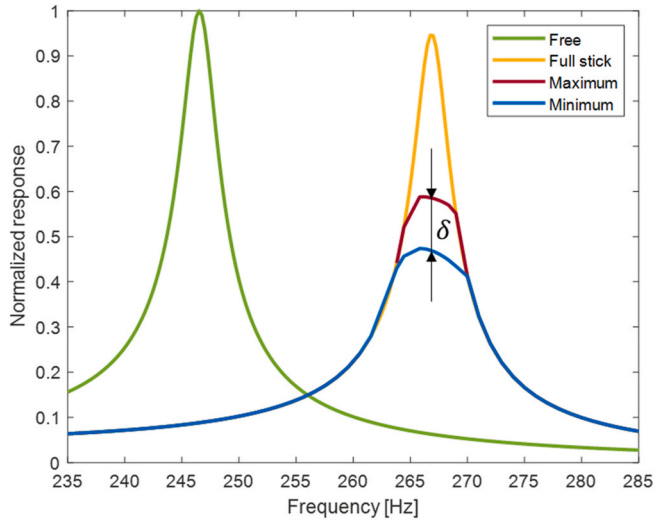

Fig. 9. Normalized response boundaries of blade 2.

damper configuration is from now on defined as *mixed configuration*. This mixed configuration determines the existence of multiple responses.

4.2. Robust design analysis

Since a response scatter δ exists in the baseline configuration (Fig. 9), a robust design analysis is here performed. Since a change in the blade geometry is an expensive process that might require multi-disciplinary investigations, the following design parameters are selected.

- Damper mass
- Damper geometry

and their effect of the robustness R of the system is analyzed separately.

4.2.1. Effect of damper mass

It is well known from the literature that the damper mass m_D strongly affects the response levels of turbine blades. In particular, the damper mass affects the amount of energy dissipated by friction, since it affects the value of centrifugal force

$$F_C^0 = m_D r_D \Omega^2$$

that keeps the damper in contact with the blade platforms, where Ω is the rotational speed of the system and r_D the radial distance of the damper from the rotation axis.

In this analysis, the effect of a non-symmetric distribution of damper masses on the robustness of the system is investigated. In particular, the centrifugal forces that act on the two dampers are defined as

$$\begin{cases} F_{C,1}^0 = F_{C.ref}^0(1-\gamma) \\ F_{C,2}^0 = F_{C.ref}^0(1+\gamma) \end{cases}, \tag{11}$$

where the design parameter γ is used to break the symmetry of the baseline system ($\gamma = 0 \rightarrow$ baseline system, $\gamma \neq 0$ different mass for the two UPDs).

First a manual search of the robust design is performed. The minimum and maximum responses are computed with the optimization algorithm described in Section 2 at different values of γ in the range [0, 0.43] and robustness is computed (Fig. 11) at each value of γ. It is observed that the robustness of the system grows with γ in a monotonic way, up to $R = 1$ at $\gamma = 0.43$.

In order to correlate the robustness of the system to the contact states on the dampers sides, the periodic contact forces at resonance are plotted for $\gamma = 0.3$ and $\gamma = 0.43$.

For $\gamma = 0.3$ (Fig. 12), both sides of the damper #1 (contacts #1 and #2) always alternate stick-slip states. This implies that the existence of multiple responses $(R < 1)$ does not depend on the damper #1.

On the contrary, a mixed configuration of the damper #2 still exists at the minimum response, showing that the existence of a mixed configuration on one damper is enough to establish multiple balance conditions and thus multiple response levels, although with an increase of robustness with respect to the baseline system ($\gamma = 0$).

For $\gamma = 0.43$ (Fig. 13), $R = 1$, in both cases, damper #1 alternate

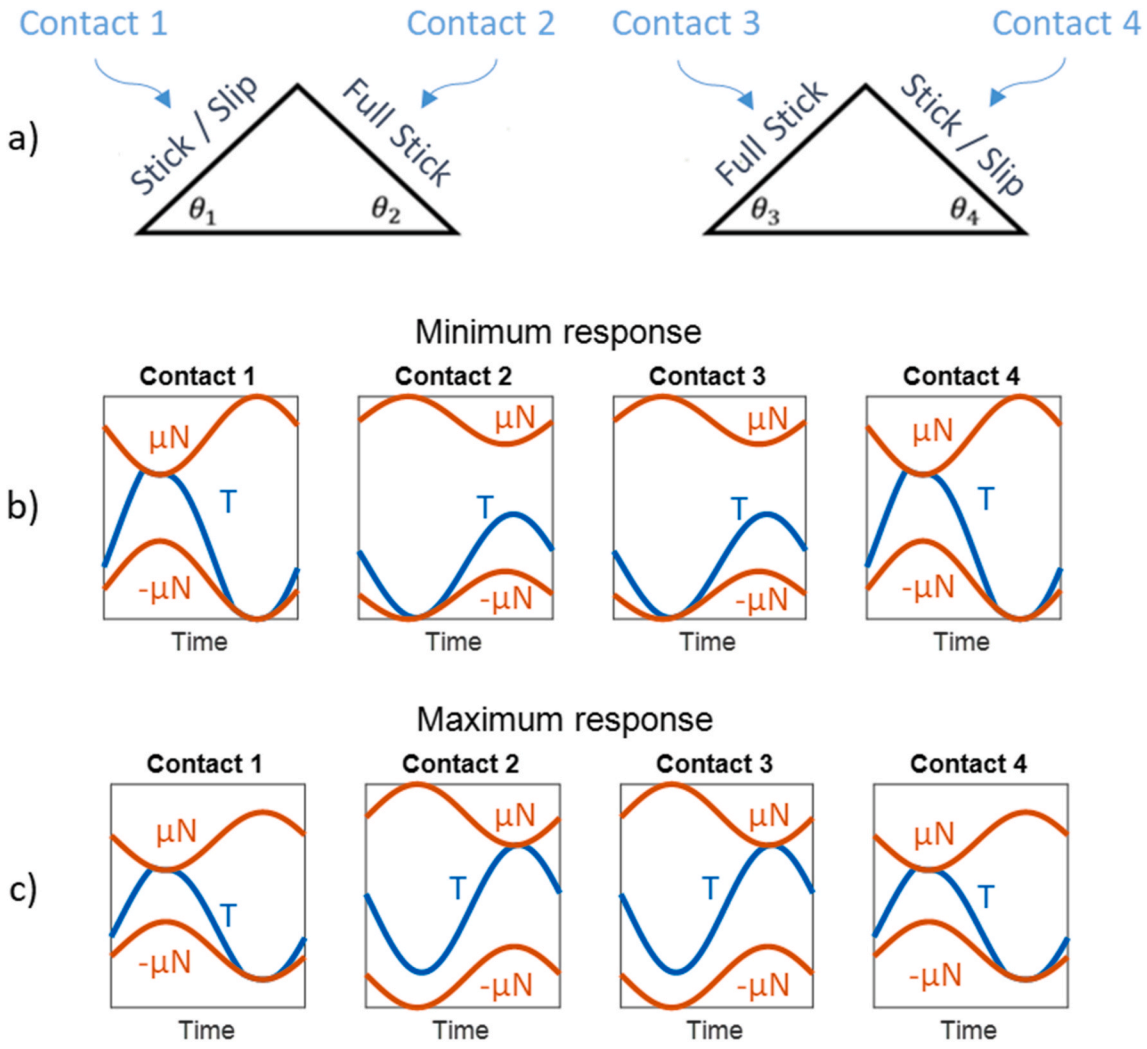

Fig. 10. a) Dampers view and contact states for baseline configuration near resonance - b) Contact forces time history near resonance for minimum response - c) Contact forces time history near resonance for maximum response.

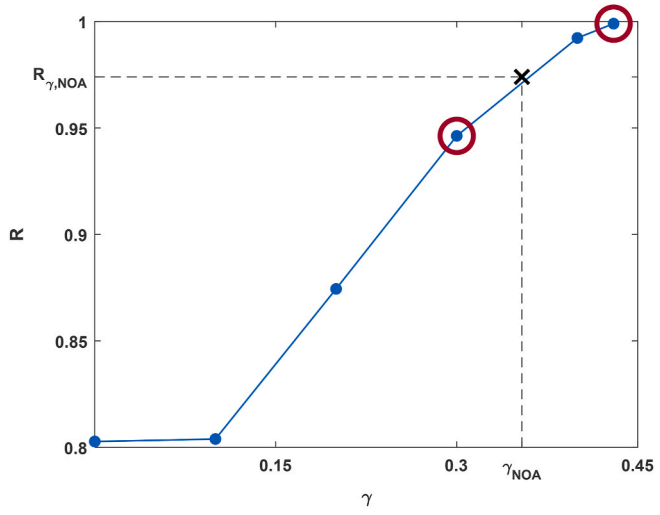

Fig. 11. $\gamma - R$ plot.

stick-slip on both sides, while both sides of damper #2 are in full-stick. In particular, the periodic forces on damper #2 (full-stick) are characterized by different static values T^0, that do not affect the dynamic balance of damper #1, that dissipates the same amount of energy in both cases, resulting in a unique response ($R = 1$). This observation suggests that the blades uncouple the dampers, preventing the mutual interactions between adjacent dampers, that could lead to multiple responses.

Again, as in the previously analyzed cases, results confirm that the mixed configuration of one or more dampers is the requirement for multiple responses.

The NOA is eventually applied to the system with $p = \gamma$, determining, as the most robust configuration, the value of $\gamma_{NOA} = 0.354$ (Fig. 11), corresponding to a robustness $R_{\gamma,NOA} = 0.974$.

Although the configuration associated to the maximum robustness ($R = 1$ @ $\gamma = 0.43$) is not found by the NOA, the difference is less than 3% and this result is considered excellent. Further analyses performed by using a different initial guess for the solution and/or using a different type of optimization strategy other than the gradient-based one, are not deemed necessary.

4.2.2. *Effect of damper geometry*

As shown in Fig. 8, damper geometry is defined by the basis angles θ_n. In the baseline configuration, symmetric dampers are used. Here the effect of the damper asymmetry on the robustness of the system is investigated. The design parameter is β and it is used to modify the basis angles in the following way:

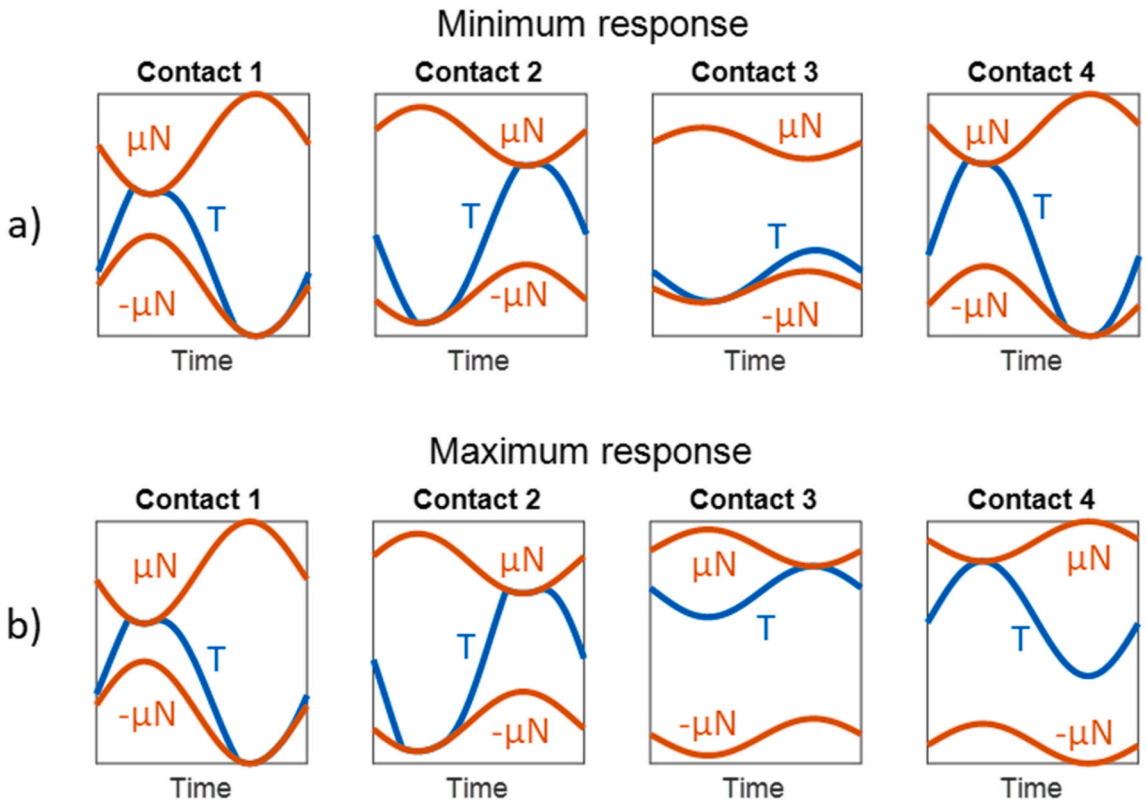

Fig. 12. $\gamma = 0.3$ – Contact Forces Time History near resonance for a) Minimum response and b) Maximum response.

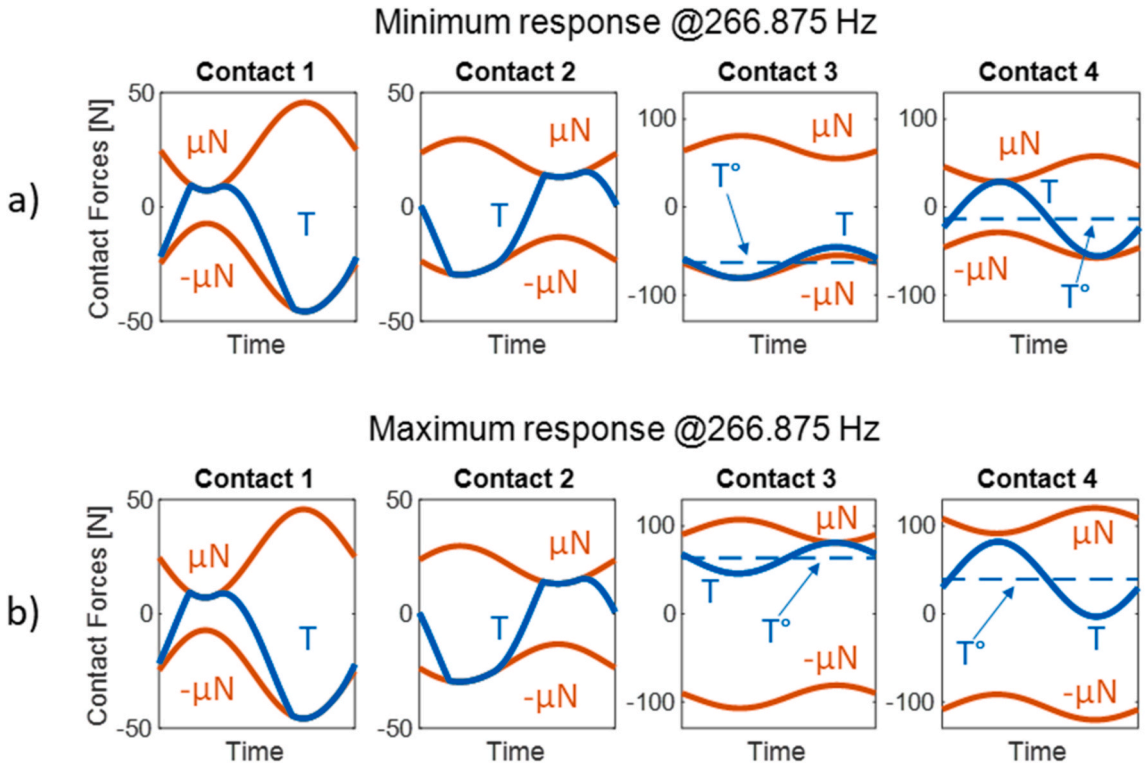

Fig. 13. $\gamma = 0.43$ – Contact Forces Time History near resonance.

$$\begin{Bmatrix} \theta_1 \\ \theta_2 \\ \theta_3 \\ \theta_4 \end{Bmatrix} = \theta_{ref} \begin{Bmatrix} 1-\beta \\ 1+\beta \\ 1+\beta \\ 1-\beta \end{Bmatrix} \tag{12}$$

where the case $\beta = 0$ corresponds to the baseline system, while $\beta \neq 0$ means non-symmetric dampers.

Also in this case, first a manual search of the robust design is performed. The minimum and maximum responses are computed with the optimization algorithm described in Section 2 at different values of β in the range [0, 0.2] and robustness is computed (Fig. 14) at each value of β. It is observed that the response is unique (R = 1) when $0.075 \leq \beta \leq 0.15$.

Also in this case, to correlate the robustness of the system to the contact states on the dampers sides, the periodic contact forces at resonance are plotted for $\beta = 0.1$ are investigated (Fig. 15). It is observed that all damper sides alternate stick-slip, justifying the computed unique response.

When $\beta < 0.075$ robustness of the system monotonically grows with β and the time histories of the periodic contact forces are similar to those of the baseline system (Fig. 10).

When $\beta > 0.15$ robustness of the systems monotonically decreases with β. A set of representative time histories of periodic contact forces ($\beta = 0.175$) are shown in Fig. 16, where mixed configuration occurs again for both dampers, but differently from the baseline configuration, now inner contacts (2 and 3) alternate stick-slip, while outer contacts (1 and 4) are in full-stick.

Results suggest that a moderate asymmetry on the dampers increase robustness, while a large asymmetry leads again to multiple responses.

Assuming as design parameter the damper angles (i.e. β), the NOA gives as a result $\beta = \beta_{NOA} = 0.0794$, which is inside the range where the robustness is maximum (R = 1). In this case the NOA was able to exactly find one of the system configurations associated to the maximum robustness R.

For both cases (mass parameter γ and geometric parameter β), NOA is proved to be a good tool in finding the parameter value that gives the maximum robustness, proving to be a sound alternative to a lengthy manual search. NOA is particularly effective in the case where the robustness (as a function of the chosen parameter) has a maximum and is not monotonic (as in the case of the β parameter).

The obtained results give also an insight into the correlation between the response scatter and the contact states over the dampers sides. The results confirm that the presence of a mixed configuration is the necessary condition to have a response scatter. In particular, the presence of a mixed configuration on each damper (Figs. 10 and 16) determines the presence of a response scatter $\delta \neq 0$, while a system-level mixed configuration, where some dampers are fully stuck while others alternate stick-slip (Fig. 12) is not enough, showing that the main structures (i.e. the blade) uncouple the dampers.

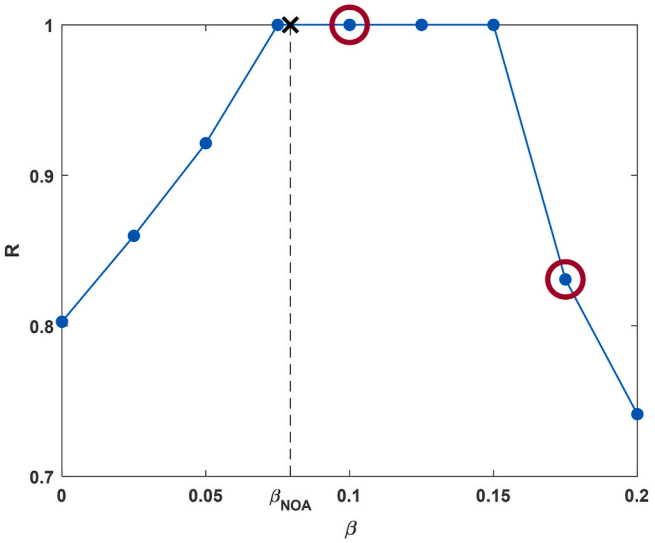

Fig. 14. $\beta - R$ plot.

5. Conclusion

The paper is focused on the robustness of turbine blades with friction contacts, whose dynamics is known to be characterized by multiple forced response levels, associated to non-unique static equilibria.

In this paper, the systematic approach originally used to determine the response boundaries ([29]) has been extended to search the most robust configuration of the system, corresponding to the minimum scatter between the maximum and the minimum response.

In particular a Nested Optimization Algorithm (NOA) is proposed as an alternative to the more computationally expensive approach, where the design space is explored manually.

The assembly of interest, in the present work, is a turbine blade array modeled as lumped masses with interposed UPDs. Despite the simplicity of this new test case, the authors believe that the analysis performed in the present work leads to useful observations that pave the way for calculations on more complex and realistic structures.

A baseline configuration of the assembly is considered and a scatter in the response is observed. A particular configuration, here called "mixed configuration", is present on both dampers; the “mixed configuration” is the condition when the damper has one side in full-stick and the other alternating stick and slip. A robust design analysis is then performed selecting the damper mass and the damper geometry (i.e. damper angles) as design parameters. The following considerations can be drawn.

1. When the damper mass is used as a design parameter:
   a. By introducing a progressive asymmetry in the mass of the two dampers, the robustness increased monotonically due to the progressive disappearance of the mixed configuration of both dampers.
   b. The NOA allowed to compute an almost optimum design configuration ($R = 0.973$).
2. When the damper geometry is used as a design parameter:
   a. By introducing a progressive asymmetry in the angles of the damper basis, the robustness did not change monotonically and it showed a maximum in a given range of values of the design parameter.
   b. When R < 1, the scatter of the response is associated to the to mixed configuration of both dampers.
   c. The NOA allowed to compute the optimum design configuration ($R = 1$).
3. In all the simulations, the scatter in the response is always associated to a mixed configuration of at least one of the two dampers.
4. The blade in the middle of the assembly proved to be able to uncouple the two dampers: any uncertainty in the static equilibrium of one damper does not influence the behavior of the other one.

CRediT authorship contribution statement

Gianmarco Zara: Conceptualization, Data curation, Formal analysis, Investigation, Methodology, Software, Writing – original draft, Writing – review & editing. **Erhan Ferhatoglu:** Conceptualization, Methodology, Writing – review & editing. **Teresa Maria Berruti:** Conceptualization, Methodology, Supervision, Writing – review & editing. **Stefano Zucca:** Conceptualization, Methodology, Supervision, Writing – review & editing.

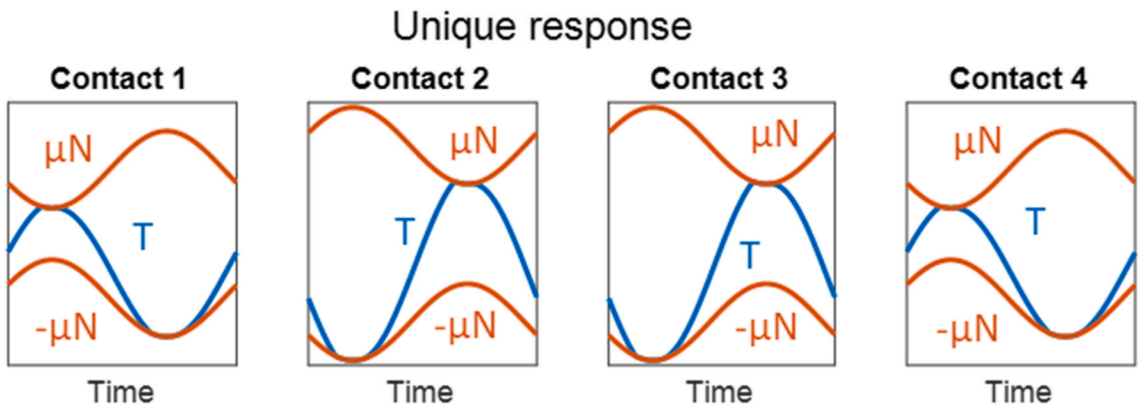

Fig. 15. $\beta = 0.1$ – contact forces time history near resonance.

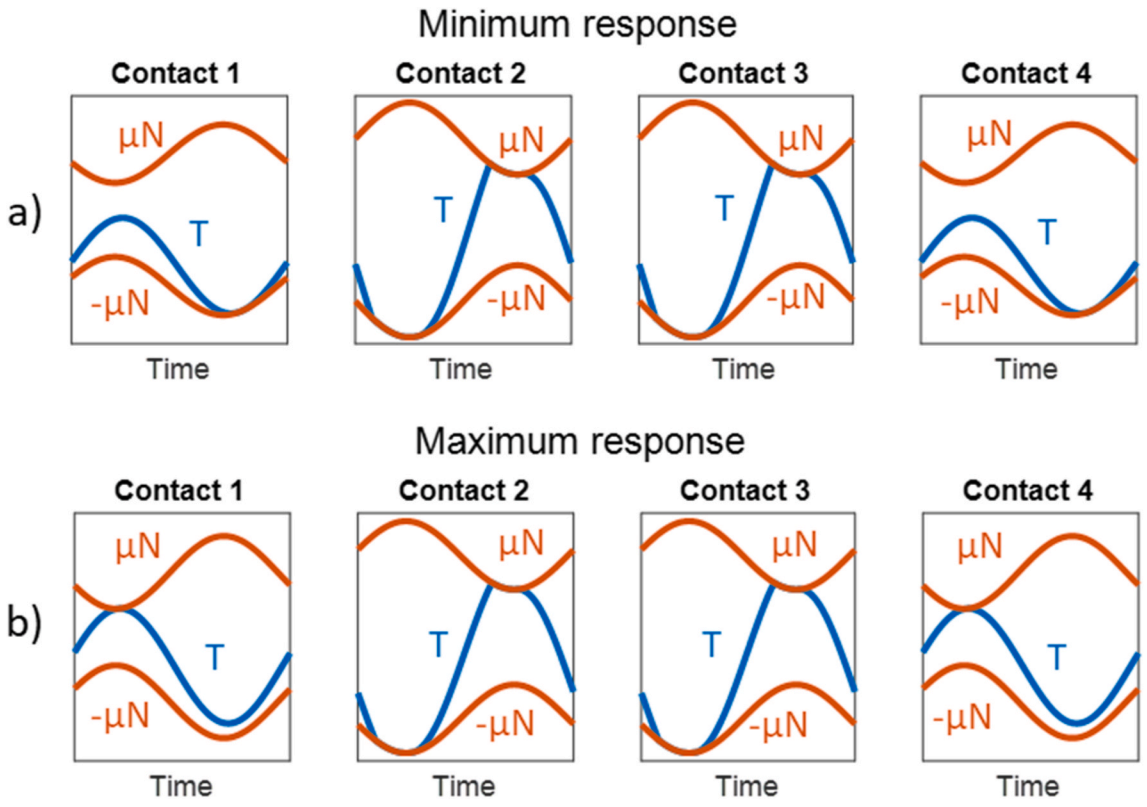

Fig. 16. $\beta = 0.175$ – contact forces time history near resonance.

Declaration of competing interest

The authors declare that they have no known competing financial interests or personal relationships that could have appeared to influence the work reported in this paper.

Data availability

No data was used for the research described in the article.

References

[1] B.A. Cowles, High cycle fatigue in aircraft gas turbines—an industry perspective, Int. J. Fract. 80 (2) (1996) 147–163, https://doi.org/10.1007/BF00012667.
[2] K.Y. Sanliturk, D.J. Ewins, A.B. Stanbridge, Underplatform dampers for turbine blades: theoretical modeling, analysis, and comparison with experimental data, J. Eng. Gas Turbines Power 123 (4) (2001) 919–929, https://doi.org/10.1115/1.1385830.
[3] E. Cigeroglu, N. An, C.-H. Menq, Forced response prediction of constrained and unconstrained structures coupled through frictional contacts, J. Eng. Gas Turbines Power 131 (2) (2009), https://doi.org/10.1115/1.2940356, 22505-022505 (11).
[4] L. Pesaresi, L. Salles, A. Jones, J.S. Green, C.W. Schwingshackl, Modelling the nonlinear behaviour of an underplatform damper test rig for turbine applications, Mech. Syst. Signal Process. 85 (2017) 662–679, https://doi.org/10.1016/j.ymssp.2016.09.007.
[5] D. Laxalde, F. Thouverez, J.-P. Lombard, Forced response analysis of integrally bladed disks with friction ring dampers, J. Vib. Acoust. Trans. ASME 132 (Feb) (2010), https://doi.org/10.1115/1.4000763.
[6] W. Tang, B. Epureanu, Nonlinear dynamics of mistuned bladed disks with ring dampers, Int. J. Non. Linear. Mech. 97 (Sep. 2017), https://doi.org/10.1016/j.ijnonlinmec.2017.08.001.
[7] J. Szwedowicz, T. Secall-Wimmel, P. Dünck-Kerst, Damping performance of axial turbine stages with loosely assembled friction bolts: the nonlinear dynamic assessment, J. Eng. Gas Turbines Power 130 (3) (Apr. 2008), https://doi.org/10.1115/1.2838998.
[8] E. Ferhatoglu, S. Zucca, D. Botto, J. Auciello, L. Arcangeli, Nonlinear vibration analysis of turbine bladed disks with midspan dampers, J. Eng. Gas Turbines Power 144 (4) (2022).

[9] E.P. Petrov, D.J. Ewins, Analytical formulation of friction interface elements for analysis of nonlinear multi-harmonic vibrations of bladed disks, J. Turbomach. 125 (2) (Apr. 2003) 364–371, https://doi.org/10.1115/1.1539868.
[10] C. Siewert, L. Panning, J. Wallaschek, C. Richter, Multiharmonic forced response analysis of a turbine blading coupled by nonlinear contact forces, J. Eng. Gas Turbines Power 132 (8) (May 2010), https://doi.org/10.1115/1.4000266.
[11] E.P. Petrov, D.J. Ewins, Effects of damping and varying contact area at blade-disk joints in forced response analysis of bladed disk assemblies, J. Turbomach. 128 (2) (Sep. 2005) 403–410, https://doi.org/10.1115/1.2181998.
[12] J.H. Griffin, Friction damping of resonant stresses in gas turbine engine airfoils, J. Eng. Power 102 (2) (Apr. 1980) 329–333, https://doi.org/10.1115/1.3230256.
[13] T.M. Cameron, J.H. Griffin, R.E. Kielb, T.M. Hoosac, An integrated approach for friction damper design, J. Vib. Acoust. 112 (2) (Apr. 1990) 175–182, https://doi.org/10.1115/1.2930110.
[14] K.Y. Sanliturk, D.J. Ewins, Modelling two-dimensional friction contact and its application using harmonic balance method, J. Sound Vib. 193 (2) (1996) 511–523, https://doi.org/10.1006/jsvi.1996.0299.
[15] C.H. Menq, B.D. Yang, NON-LINEAR spring resistance and friction damping of frictional constraint having two-dimensional motion, J. Sound Vib. 217 (1) (1998) 127–143, https://doi.org/10.1006/jsvi.1998.1739.
[16] B.D. Yang, C.H. Menq, Characterization of 3D contact kinematics and prediction of resonant response of structures having 3D frictional constraint, J. Sound Vib. 217 (5) (1998) 909–925, https://doi.org/10.1006/jsvi.1998.1802.
[17] M. Krack, L. Salles, F. Thouverez, Vibration prediction of bladed disks coupled by friction joints, Arch. Comput. Methods Eng. 24 (3) (2017) 589–636, https://doi.org/10.1007/s11831-016-9183-2.
[18] C.M. Firrone, S. Zucca, M.M. Gola, The effect of underplatform dampers on the forced response of bladed disks by a coupled static/dynamic harmonic balance method, Int. J. Non. Linear. Mech. 46 (2) (2011) 363–375, https://doi.org/10.1016/j.ijnonlinmec.2010.10.001.
[19] S. Zucca, C.M. Firrone, M.M. Gola, Numerical assessment of friction damping at turbine blade root joints by simultaneous calculation of the static and dynamic contact loads, Nonlinear Dyn. 67 (3) (2012) 1943–1955, https://doi.org/10.1007/s11071-011-0119-y.
[20] B.D. Yang, C.H. Menq, Characterization of contact kinematics and application to the design of wedge dampers in turbomachinery blading: Part 1—stick-Slip contact kinematics, J. Eng. Gas Turbines Power 120 (2) (Apr. 1998) 410–417, https://doi.org/10.1115/1.2818138.
[21] B.D. Yang, C.H. Menq, Characterization of contact kinematics and application to the design of wedge dampers in turbomachinery blading: Part 2—prediction of forced response and experimental verification, J. Eng. Gas Turbines Power 120 (2) (Apr. 1998) 418–423, https://doi.org/10.1115/1.2818139.
[22] A. Klarbring, Examples of non-uniqueness and non-existence of solutions to quasistatic contact problems with friction, Ing. Arch. 60 (8) (1990) 529–541, https://doi.org/10.1007/BF00541909.
[23] J.R. Barber, A. Klarbring, M. Ciavarella, Shakedown in frictional contact problems for the continuum, Compt. Rendus Mec. 336 (1) (2008) 34–41, https://doi.org/10.1016/j.crme.2007.10.013.
[24] A.R.S. Ponter, Shakedown limit theorems for frictional contact on a linear elastic body, Eur. J. Mech. - A/Solids 60 (2016) 17–27, https://doi.org/10.1016/j.euromechsol.2016.05.003.
[25] R.C. Flicek, M.R.W. Brake, D.A. Hills, J.R. Barber, in: M.R.W. Brake (Ed.), Predicting the Shakedown Limits of Joints Subject to Fretting and High Cycle Fatigue BT - the Mechanics of Jointed Structures: Recent Research and Open Challenges for Developing Predictive Models for Structural Dynamics, Springer International Publishing, Cham, 2018, pp. 561–582, https://doi.org/10.1007/978-3-319-56818-8_31.
[26] R.C. Flicek, M.R.W. Brake, D.A. Hills, Predicting a contact's sensitivity to initial conditions using metrics of frictional coupling, Tribol. Int. 108 (2017) 95–110, https://doi.org/10.1016/j.triboint.2016.09.038.
[27] S. Zucca, C.M. Firrone, M.M. Gola, Modeling underplatform dampers for turbine blades: a refined approach in the frequency domain, J. Vib. Control 19 (2013) 1087–1102.
[28] E. Ferhatoglu, S. Zucca, Determination of periodic response limits among multiple solutions for mechanical systems with wedge dampers, J. Sound Vib. 494 (2021) 115900, https://doi.org/10.1016/j.jsv.2020.115900.
[29] E. Ferhatoglu, S. Zucca, On the non-uniqueness of friction forces and the systematic computation of dynamic response boundaries for turbine bladed disks with contacts, Mech. Syst. Signal Process. 160 (2021) 107917, https://doi.org/10.1016/j.ymssp.2021.107917.
[30] A. Cardona, T. Coune, A. Lerusse, M. Geradin, A multiharmonic method for non-linear vibration analysis, Int. J. Numer. Methods Eng. 37 (9) (May 1994) 1593–1608, https://doi.org/10.1002/nme.1620370911.
[31] A. Cardona, A. Lerusse, M. Géradin, Fast Fourier nonlinear vibration analysis, Comput. Mech. 22 (2) (1998) 128–142.
[32] M.J. Kochenderfer, T.A. Wheeler, Algorithms for Optimization, Mit Press, 2019.
[33] T.M. Cameron, J.H. Griffin, An alternating frequency/time domain method for calculating the steady-state response of nonlinear dynamic systems, J. Appl. Mech. 56 (1) (Mar. 1989) 149–154, https://doi.org/10.1115/1.3176036.
[34] C. Siewert, L. Panning, C. Gerber, P.-A. Masserey, Numerical and Experimental Damping Prediction of a Nonlinearly Coupled Low Pressure Steam Turbine Blading, Jun. 09, 2008, pp. 531–542, https://doi.org/10.1115/GT2008-51073.